Original Paper

Cellular Physiology and Biochemistry

Cell Physiol Biochem 2011;28:1009-1022

Accepted: October 04, 2011

Dissecting the Conserved NPxxY Motif of the M_3 Muscarinic Acetylcholine Receptor: Critical Role of Asp-7.49 for Receptor Signaling and Multiprotein Complex Formation

Dasiel O. Borroto-Escuela[1, 2], Wilber Romero-Fernandez[1], Gloria García-Negredo[3], Patricia A. Correia[4], Pere Garriga[1], Kjell Fuxe[2] and Francisco Ciruela[3]

[1]Centre de Biotecnologia Molecular, Department d'Enginyeria Química, Universitat Politècnica de Catalunya, Terrassa, [2]Neuroscience Department, Karolinska Institutet, Stockholm, [3]Unitat de Farmacologia, Departament de Patologia i Terapèutica Experimental, Facultat de Medicina, Universitat de Barcelona, L'Hospitalet de Llobregat, [4]W.M. Keck Centre for Integrative Neuroscience and Department of Physiology, University of California, San Francisco

Key Words

G protein-coupled receptors • Muscarinic acetylcholine receptors • NPxxY motif • Phospholipase D • Phospholipase C • Monomeric small G proteins • Desensitization

Abstract

Acetylcholine challenge produces M_3 muscarinic acetylcholine receptor activation and accessory/scaffold proteins recruitment into a signalsome complex. The dynamics of such a complex is not well understood but a conserved NPxxY motif located within transmembrane 7 and juxtamembrane helix 8 of the receptor was found to modulate G protein activation. Here by means of receptor mutagenesis we unravel the role of the conserved M_3 muscarinic acetylcholine receptor NPxxY motif on ligand binding, signaling and multiprotein complex formation. Interestingly, while a N7.49D receptor mutant showed normal ligand binding properties a N7.49A mutant had reduced antagonist binding and increased affinity for carbachol. Also, besides this last mutant was able to physically couple to $G\alpha_{q/11}$ after carbachol challenge it was neither capable to activate phospholipase C nor phospholipase D. On the other hand, we demonstrated that the Asn-7.49 is important for the interaction between M_3R and ARF1 and also for the formation of the ARF/Rho/$\beta\gamma$ signaling complex, a complex that might determine the rapid activation and desensitization of PLD. Overall, these results indicate that the NPxxY motif of the M_3 muscarinic acetylcholine receptor acts as key conformational switch for receptor signaling and multiprotein complex formation.

Introduction

The M_3 muscarinic acetylcholine receptor (M_3R) is a member of the muscarinic receptor family that controls a large array of functions in both the central and peripheral nervous systems [1]. It is a class A, rhodopsin-like, G protein-coupled receptor (GPCR) that signals through the heterotrimeric G protein $G\alpha_{q/11}$, thus activating phospholipase C_β (PLC_β) and increasing intracellular calcium [2]. M_3R regulates a network of signaling molecules, including protein kinase C (PKC), small Rho GTPase, phospholipase D (PLD), phosphoinositide-3

KARGER

Fax +41 61 306 12 34
E-Mail karger@karger.ch
www.karger.com

1015-8987/11/0285-1009$38.00/0

Accessible online at:
www.karger.com/cpb

Francisco Ciruela
Unitat de Farmacologia, Dept. de Patologia i Terapèutica Experimental
Facultat de Medicina (Campus de Bellvitge), Pavelló de Govern
Av. Feixa Llarga, s/n 08907 L'Hospitalet del Llobregat Barcelona (Spain)
Tel. +34-934024280/+34-934035820, Fax +34-934029082, E-Mail fciruela@ub.edu

kinase (PI3K), non-receptor kinases and mitogen-activated protein kinases (MAPKs) [3].

Interactions within conserved residues in the M_3R intracellular loops have been proposed to be critical in preserving normal receptor activation, G protein-coupling, signaling and trafficking [4-6]. Chimeric receptor construction together with site directed mutagenesis showed that both the M_3R second intracellular loop and the C-terminal portion of the third intracellular loop are important for coupling to the $G\alpha_{q/11}$ protein [7]. In addition, receptor activation is mediated by a conformational rearrangement that includes transmembrane helix 7 (TMH7) and probably, as described for rhodopsin, movement within the C terminal tail juxtamembrane helix 8 (HX8) [8].

Sequence alignment of GPCRs of the rhodopsin subfamily reveals that most members of this subfamily, including the M_3R, contain a widely conserved NPxxY sequence motif at the end of TMH7 [9]. Interestingly, by means of mutagenesis and molecular modeling studies based on the rhodopsin crystal structure it has been shown that this motif is involved in an interaction network that modulates receptor's expression, signaling and trafficking [10-14]. Also, based on computational studies a theoretical model that explains the special structural features of the conserved N/DP motif has been proposed. Hence, this motif differs from a regular proline kink (of an ideal α-helix), thus allowing for a major flexibility in the TMH7 [15]. Consequently, by acting as a sensitive conformational switch this NPxxY motif may play a key role in the GPCR activation selectivity and efficacy, thus determining the receptor signaling extend. In addition, this domain regulates the interaction of the receptor with accessory/scaffold proteins, thus controling the formation of the receptor signalosome. Indeed, interaction between M_3R and small monomeric G proteins, for instance ADP-ribosylation factors (ARFs) and Ras homolog gene family member A (RhoA), has been described as critical during the activation of the PLD and ROCK pathway [16-19]. Thus, based on the fact that NPxxY motif is involved in the activation and signalsome complex formation of some GPCRs we wanted to know the precise function of this motif in the M_3R. Therefore, two mutants were generated, namely the Asn at position 540 (N7.49) and located within the conserved NPxxY motif was replaced by Asp (N7.49D) and by Ala (N7.49A). Mutation of Asn, to Ala switches the M_3R to a high affinity inactive conformation unable to signal properly. However, the mutated receptor keeps the ability to form stable complexes with $G\alpha_{q/11}$ protein in response to agonist-stimulation, as demonstrated by means of co-immunoprecipitation experiments. On the other hand, the N7.49D mutant ($M_3R^{N7.49D}$) showed a unlike activation time-course and desensitization profile when compared to the M_3R^{wt}. Also, by means of co-immunoprecipitation experiments we corroborated that this mutant uses a non ARF1-mediated pathway to activate/desensitize the PLD. Overall, we showed that the conserved Asn residue within the NPxxY motif of the M_3R determines the ability to form stable complexes with different populations of G proteins ($G\alpha_{q/11}$ and $G\alpha_{12/13}$) and small monomeric G proteins (ARF1, ARF6 and RhoA), thus determining the activation/desensitization profile of the signaling pathways in which this receptor partake.

Materials and Methods

Materials

Dulbecco's modified Eagle's medium, penicillin/streptomycin and fetal bovine serum were purchased from Invitrogen (Carlsbad, CA, USA). [^{35}S]-GTPγS (1,202 Ci/mmol), [^{3}H]-myo-inositol (3.0 Ci/ml) and N-[^{3}H]-methyl scopolamine ([^{3}H]-NMS, 81 Ci/mmol), were from Amersham Biosciences (Piscataway, NJ, USA). Restriction enzymes were from New England Biolabs (Beverly, MA, USA). Carbamylcholine chloride (carbachol, CCh), atropine sulphate and all other reagents were purchased from Sigma-Aldrich (St. Louis, MO, USA).

Plasmid constructs

The constructs presented here were made using standard molecular biology techniques employing PCR and fragment replacement strategy. The cDNAs for the human M_3R (kindly provided by T. Bonner, NIH, USA) was subcloned into the mammalian expression vector pcDNA-3.1 (Invitrogen) containing three hemagglutinin (HA) epitopes (pcDNA3.1-3xHA; gift from P. Calvo, SFU, CA, USA), thus resulting in the pcDNA3.1-3xHA-M_3R vectors. Briefly, 1.9-kb fragment encoding the human M_3R was amplified using sense and antisense primers harboring unique *Eco*RV and *Xba*I sites and then subcloned into *Eco*RV/*Xba*I sites of the mammalian pcDNA3.1-3xHA vector. The Asn of the M_3R NPxxY motif was exchange to Asp and Ala by using the QuikChange site directed mutagenesis kit from Stratagene (La Jolla, CA, USA). The sense primers used were: $FM_3R^{N7.49D}$ (5'-ACC TCT CTG GCT GTC CTA CTC ACC-3'); $FM_3R^{N7.49A}$ (5'-CTG TTT CTG CTG GGC CCC CGC CTT TG-3'). The cDNA encoding the human GPR37 receptor was purchased from GenomeCube® (imaGenes, Berlin, Germany), amplified and subcloned into pcDNA-3.1. The reading frame, PCR integrity of the cloned constructs and the sequences of the mutants were confirmed by DNA sequencing. Finally, amino-acid residues along the human M_3R sequence were numbered according the most conserved residue in the TMH and thus following the consensus-numbering scheme described by Ballesteros et al. [20].

Cell culture and transfection

COS-7 cells were maintained in Dulbecco's modified Eagle's medium supplemented with 10% fetal calf serum (FCS), 100 U/ml streptomycin, 100 µg/ml penicillin, 2 mM L-glutamine (all from Invitrogen) at 37°C in a humidified 5% CO_2 incubator. For transfection, 2×10^6 cells were seeded into 100-mm dishes. About 24 h later, cells were co-transfected with pcDNA3.1-3xHA-M_3R vector or mutants, by using the Lipofectamine™ Plus reagent (Invitrogen).

RNA Interference and immunofluorecence analysis

A pool of six different double-stranded siRNAs targeting ARF-1 were designed by and obtained from Santa Cruz Biotechnology (sc-141186, Stockholm, Sweden) and Selleck (ARF1 siRNA kit, TX, USA). A siRNA duplex with an irrelevant sequence (siRNA negative control, Selleck, TX, USA) was used as a control. Thus, COS-7 cells were transfected with 20 µM siRNA using Oligofectamine (Invitrogen) according to the manufacturer's instructions and transfection was repeated 24h later. Then, the next day cells were challenged with CCh at the indicated times and processed for ARF1 immunostaining and PLD activity determinations. In brief, for ARF1 immunostaining cells were labelled with the rabbit anti-ARF1 monoclonal antibody (Abcam, Stockholm, Sweden) and then a secondary anti-rabbit antibody coupled to Alexa-Fluor 488 (Molecular Probe, Stockholm, Sweden). Immunofluorescence analysis was carried out by using a 63× oil immersion objective in a Leica TCS-SL confocal microscope (Leica, USA). Images obtained from ten cells (two different experiments) were analyzed for each condition (control and ARF-1 depleted cells in 0, 15, 30 min CCh treated cells). For each image the average fluorescence intensity per field was examined.

Membrane preparation and radioligand binding assay

About 48 h after transfection, COS-7 cells were washed twice with cold phosphate-buffered saline (PBS; pH 7.4), harvested and homogenized in binding buffer (25 mM sodium phosphate, 5 mM $MgCl_2$, pH 7.4), using a Polytron tissue homogeniser. Cell membranes were collected by centrifugation at 20000xg for 15 min and homogenized as above. After centrifugation at 40000xg for 20 min at 4°C, the final pellet was resuspended in binding buffer, and membranes were either used immediately or frozen in liquid nitrogen and stored at -80°C until needed. Protein concentration was determined by using the Bradford protein assay kit (Bio-Rad, Hercules, CA, USA). To determine the affinity of NMS for each sample, membranes were incubated with different concentrations of [^{3}H]-NMS (ranging from 12.5 pM to 1.5 nM) in binding buffer at 25°C for 60 min. Incubations were stopped by filtration through Whatman (Maidstone, Kent, UK) GF/B filters and washed extensively with ice-cold PBS before scintillation counting. Nonspecific binding was determined in the presence of 10 µM atropine. Agonist binding potencies were determined by means of competition with [^{3}H]-NMS. Briefly, membranes were incubated with 0.1 nM [^{3}H]-NMS and concentrations ranging from 10 pM to 10 mM of CCh in binding buffer at 25°C for 3h. Agonist binding studies were carried out without GTP and GTP analogues; because previous studies had shown that such agents did not affect the agonist binding properties of the M_3R when transiently expressed in COS-7 cells [21]. Assays were stopped by filtration and samples were subject to scintillation counting, as described above.

PLD and PLC assay activities

PLD and PLC activities were recorded as accumulation of [^{3}H]phosphatidylbutanol ([^{3}H]PtdBut) and [^{3}H]inositol phosphate ([^{3}H]IP), respectively [22]. Briefly, transfected COS-7 cells growing in 12-well plates were metabolically labeled with [^{3}H]palmitate (2 µCi/well, Amersham Biosciences) and [^{3}H]myoinositol (3 µCi/ml, Amersham Biosciences) in inositol-free DMEM (Invitrogen) during 18-24 h. For [^{3}H]IP determinations agonist (CCh) response were measured usually over 40-60 min in the presence of 10 mM LiCl before cells were lysed in ice-cold 10 mM formic acid. [^{3}H]IP was separated on Dowex AG1-X8 ion exchange columns (Bio-Rad, Hercules, CA, USA). For [^{3}H]PtdBut determinations agonist (CCh) response was measured usually over 30-40 min in the presence of 30 mM butan-1-ol, then phospholipids were extracted into chloroform/methanol and [^{3}H]PtdBut was separated on Whatman LK5D thin layer chromatography plates (Whatman). For desensitization experiments, in both assays, prelabeled cells were treated 2 min with agonist in Hank's Buffered Salt Solution (HBSS), and then washed twice with HBSS (15 mM HEPES, 118 mM NaCl, 5 mM KCl, 1 mM $CaCl_2$, 1 mM $MgCl_2$, and 5Mm D-glucose, pH 7.4). Then, agonist was added in the conditions described above for the indicated periods of time. Inhibitory agents and the butan-1-ol were added 30 min before and immediately after agonist addition, respectively. For assays in acute permeabilized cells, prelabeled COS-7 cells were incubated with agonist (100 µM CCh) or vehicle for 10 min at 37°C before intracellular buffer was added (2 mM MgATP, 10 µM NAD, 8 µM digitonin, and 30 mM butan-1-ol) in the presence or absence of Brefeldin A (BFA) or C3 exoenzyme (C3). Data from scintillation counting of 4 to 6 independent experiments were expressed as means ± S.E.

When indicated, PLD activity was also evaluated by the Amplex Red Phospholipase D assay kit (Molecular Probes, Stockholm, Sweden) used according to the manufacturer's instructions. Briefly, transiently transfected COS-7 cells were washed 3 times with phosphate-buffered saline and then incubated overnight in basal medium containing 5 mg/mL bovine serum albumin (BSA) and antibiotics. Cells were challenged with CCh (10 µM) during 15 and 30 min. The basal level of constitutive PLD activity was determined in the absence of CCh. Next, cells were washed with and kept in 300 µL with ice-cold 50 mM Tris, pH 8.0, containing 1 mM EGTA and complete protease inhibitor cocktail without ethylenediaminetetraacetic acid (Roche, Stockholm, Sweden). Cells were lysed by 3 freeze-thaw cycles, collected and mixed 1:1 (v/v) with Amplex Red reaction buffer (Amplex Red Phospholipase D assay kit; Molecular Probes), and PLD activity was measured as a fluorescence signal after 30 minutes incubation at 37°C in a POLARstar Optima plate reader (BMG Labtech, Offenburg, Germany).

[^{35}S]-GTPγS binding assay

COS-7 cell membranes were diluted in an ice-cold buffer containing 10 mM HEPES and 0.1 mM EDTA, 5 Mm deoxycholate, pH 7.4. Samples were subsequently pelleted and resuspended in a binding buffer consisting of 10 mM HEPES, 10 mM $MgCl_2$, 100 mM NaCl, pH 7.4 at a final protein concentration of 125 µg/ml. Incubations were conducted in a final assay volume of 1 ml (125 µg total protein) for 1 h at 30°C in the presence of 1 µM GDP and 0.3 nM [^{35}S]-GTPγS (Amersham Biosciences) and the suitable ligand concentration (CCh from 1 nM to 1 mM). The reaction was stopped by addition of 5 ml of ice-cold buffer containing 10 mM HEPES/NaOH, 1 mM $MgCl_2$, pH 7.4 followed by rapid filtration through glass fibre filters GF/C filters (Whatman) presoaked in the same buffer. The filters were washed twice with 5 ml of ice-cold buffer and the radioactivity was measured by scintillation counting. Nonspecific binding was determined in the presence of 10 µM GTPγS. Assays were performed in triplicate.

Co-immunoprecipitation and Western blot experiments

Immunoprecipitation and western blot experiments were carried out as described previously [23]. Briefly, to immunoprecipitate M_3R constructs and its associated proteins, plasmids encoding the 3xHA-M_3R constructs and the $G\alpha_{q/11}$, $G\alpha_{12/13}$, RhoA^{GFP}, ARF1^{GFP} or ARF6^{GFP} expressing vectors were transiently co-transfected into COS-7 cells. After 48 h cells were serum-deprived for 4 h and then incubated in the absence or presence of 10 µM of CCh for 10 min. After a washing with cold PBS the cells were solubilized with 4 mM CHAPS and processed for immunoprecipitation using a mouse anti-HA monoclonal antibody (A01244, 1 µg; Genscript, Hong Kong). Proteins transferred onto PVDF membranes were immunodetected by using a goat anti-HA polyclonal antibody (A00168, 1:1000; Genscript), rabbit anti-$G\alpha_{q/11}$ polyclonal antibody (sc-392, 1:1000; Santa Cruz Biotechnology), rabbit anti-$G\alpha_{12/13}$ polyclonal antibody (s-20, 1:300; Santa Cruz Biotechnology) and rabbit anti-GFP polyclonal antibody (A01388, 1: 10000; Genscript) as primary antibodies; and then horseradish-peroxidase (HRP)-conjugated goat anti-rabbit IgG (1:60000; Pierce, Rockford, IL, USA) and horseradish-peroxidase (HRP)-conjugated mouse anti-goat IgG (1:30000; Pierce) as secondary antibodies, and developed using SuperSignal West Pico Chemiluminescent Substrate (Pierce).

MAPK assay

Transiently transfected COS-7 cells expressing M_3R subtype were grown to 80% confluence and rendered quiescent by serum starvation overnight before MAPK phosphorylation assay. Subsequently, further 2h incubation in fresh serum-free medium was performed to minimize basal activity. Then, cells were stimulated by adding medium containing the muscarinic agonist CCh (10 µM). Rapid rinsing, with ice-cold PBS finished stimulation, and cell lyses was performed during 10 min by adding 500 µl ice-cold lyses buffer (50 mM Tris-HCL, pH 7.4, 150 mM NaCl, 1% TritonX-100, protease and phosphatase inhibitor cocktail). The cellular debris was removed by centrifugation at 13000xg for 5 min at 4°C, and the total protein content was measured using BCA Protein Assay Reagent (Pierce). Aliquots corresponding to 5 µg of protein were mixed with sodium dodecyl sulphate (SDS) loading buffer, applied to 12% SDS-polyacrylamide gel electrophoresis (SDS-PAGE) and analyzed by Western blot. Extracellular signal regulated kinase 1/2 (ERK1/2) activation was assayed by incubating PVDF blots with a mouse anti-phospho-ERK1/2 monoclonal antibody (Sigma-Aldrich). Control blots were also run in parallel and probed with rabbit anti-ERK1/2 polyclonal antibody (Sigma-Aldrich) that recognized both unphosphorylated and phosphorylated forms. The immunoreactive bands were visualized as described above and then measured by quantitative densitometry.

Data analysis

All binding data were analyzed using the GraphPad PRISM 4.0 software (GraphPad Prism, San Diego, CA, USA). Basal binding was defined as [^{35}S]-GTPγS binding without agonist in the [^{35}S]-GTPγS binding assay. For each agonist concentration, the percentage of binding over basal was calculated to find out the agonist-stimulated [^{35}S]-GTPγS binding. Data were fit to a sigmoidal dose-response curve. For statistical evaluation of the biochemical data, unless otherwise mentioned, one-way analysis of variance (ANOVA) was used. Group differences after significant ANOVAs were measured by post hoc Bonferroni´s Multiple Comparison test.

Results

In order to unravel the structural and functional role of the M_3R NPxxY motif we performed mutagenesis experiments. Thus, the Asn of this conserved domain along muscarinic acetylcholine receptors (Fig. 1) was replaced by aspartic acid (Asp; N7.49D) and by alanine (Ala; N7.49A). Subsequently, agonist and antagonist binding determinations, phosphoinositide hydrolysis stimulation, G protein activation and co-immunoprecipitation experiments with monomeric small and heterotrimeric G proteins were performed after transient expression of these receptor constructs into COS-7 cells.

Ligand binding properties of the NPxxY motif mutants

M_3R^{wt}, $M_3R^{N7.49D}$ and $M_3R^{N7.49A}$ were transiently expressed in COS-7 cells and assayed for their ability to bind receptor agonist and antagonist. The results of radioligand binding experiments are summarized in Table 1. In brief, saturation binding experiments showed that the $M_3R^{N7.49D}$ mutant was expressed at a density comparable to that observed for the M_3R^{wt}, however the $M_3R^{N7.49A}$ mutant showed a four-fold reduction in the maximum binding capacity (B_{max}; Table 1). In addition, all

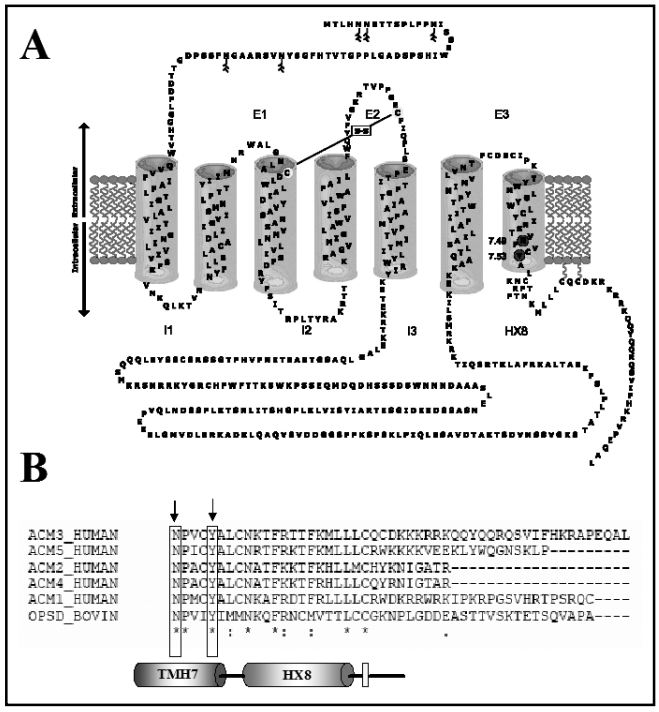

Fig. 1. Location of the NPxxY motif in the M_3R helix net representation. A. Schematic two-dimensional model of the human M_3R. The extracellular domain is located on top and the intracellular domain at the bottom. The extracellular (E) and intracellular (I) loops together with the putative juxtamembrane helix 8 (HX8) are shown. Also, the mutated residue (N7.49) within the NPxxY motif is highlighted (grey filled encircled residue). Finally, the putative extracellular disulfide bond and the glycosylation and palmitoylation sites are also depicted. B. Schematic representation of the multiple alignments of the NPxxY motif of the human muscarinic acetylcholine receptor family (ACM1 to ACM5) and bovine rhodopsin (OPSD). Residues that form part of the NPxxY motif at the end of TMH7 (blue cylinder) are shown in a grey filled box. The arrow denotes the position of the Asn-7.49 within the NPxxY motif. Also, the conserved residues among the family are depicted with an asterisk and the putative HX8 is also shown (red cylinder).

receptor mutants displayed an affinity for the NMS antagonist similar to that observed by M_3R^{wt} (Table 1). On the other hand, when the agonist binding parameters were assessed the $M_3R^{N7.49D}$ showed similar affinity for carbachol when compared with M_3R^{wt} but the $M_3R^{N7.49A}$ showed a ~7.6 fold-increment in affinity, thus suggesting that the Asn→Ala substitution increases the affinity of the receptor for carbachol.

The $M_3R^{N7.49A}$ is unable to activate the PLC, the PLD and the MAPK pathway

Next, we explored the functionality of each receptor mutant expressed in COS-7 cells by quantifying the

	[^{3}H]-NMS Binding		Carbachol Binding
Receptor construct:	K_D (pM)	B_{max} (fmol/mg)	K_{app} (μM)
3xHA-M_3R^{wt}	90 ± 17	924 ± 37	8.4 ± 2.3
3xHA-$M_3R^{N7.49D}$	87 ± 15	910 ± 33	12.2 ± 2.8
3xHA-$M_3R^{N7.49A}$	105 ± 69	226 ± 33¶	1.1 ± 0.8¶

Table 1. Ligand binding properties of M_3R constructs*. *Radioligand binding studies on COS-7 cell membranes expressing wild type M_3R (3xHA-M_3R^{wt}) or M_3R mutants (3xHA-$M_3R^{N7.49D}$ and 3xHA-$M_3R^{N7.49A}$) were carried out as described under Materials and methods. Curves were better fitted by non-linear regression analysis assuming a single binding site. K_D values were determined by using GraphPad Prism software. K_{app} values were calculated from IC_{50} values using Cheng and Prussof equation and can be consider an estimation of K_i values. Hill coefficients (nH) was significantly smaller than 1 ($P< 0.05$). ¶$p<0.05$ when compared to COS-7 cells expressing 3xHA-M_3R^{wt} or 3xHA-$M_3R^{N7.49D}$. Results represent mean ± S.E. (n = 5).

activation of the main signaling pathways activated by the M_3R, namely the PLC, the PLD and the MAPK pathway [3]. M_3R-mediated PLC stimulation has been extensively described and constitutes one of the main pathways activated by this muscarinic acetylcholine receptor subtype after agonist challenge [24, 25]. In order to assess the ability of wild type and mutant receptors to activate the PLC-signaling cascade, we measured the total inositol phosphates (IP) accumulation. As expected, the M_3R^{wt} stimulation produced a dose-dependent accumulation of IP with an EC_{50} of 3.4±0.5 μM (Fig. 2A). Also, the $M_3R^{N7.49D}$ showed a similar dose-response curve of IP accumulation (EC_{50}=3.6±0.2 μM; Fig. 2A). Interestingly, under similar experimental conditions no significant agonist-mediated IP accumulation was observed in cells expressing the $M_3R^{N7.49A}$ (Fig. 2A).

Although the most established M_3R signaling pathway is the pertussis toxin-insensitive activation of PLC via the heterotrimeric $G\alpha_{q/11}$ protein, PLD is also strongly activated via both the $G\alpha_{q/11}$ and $G\alpha_{12/13}$ proteins [26, 27]. We then studied the ability of the M_3R^{wt} and the mutant receptors to activate PLD as measured by the formation of phosphatidylbutanol (PtdBut). Interestingly, while the M_3R^{wt} and the $M_3R^{N7.49D}$ had a similar pattern of PLD activation (EC_{50}=1.4±0.6 μM and 1.2±0.3 μM, respectively) the $M_3R^{N7.49A}$ was unable to activate PLD even when exposed to 1 mM of CCh (Fig. 2B). Finally, to rule out that the measured EC_{50} and E_{max} changes were due to changes in receptor density we plotted the negative logarithm of EC_{50} *vs.* the M_3R^{wt} and $M_3R^{N7.49D}$ density. This plot showed that while the receptor expression could be slightly variable the EC_{50} shift was independent of receptor density (data not shown).

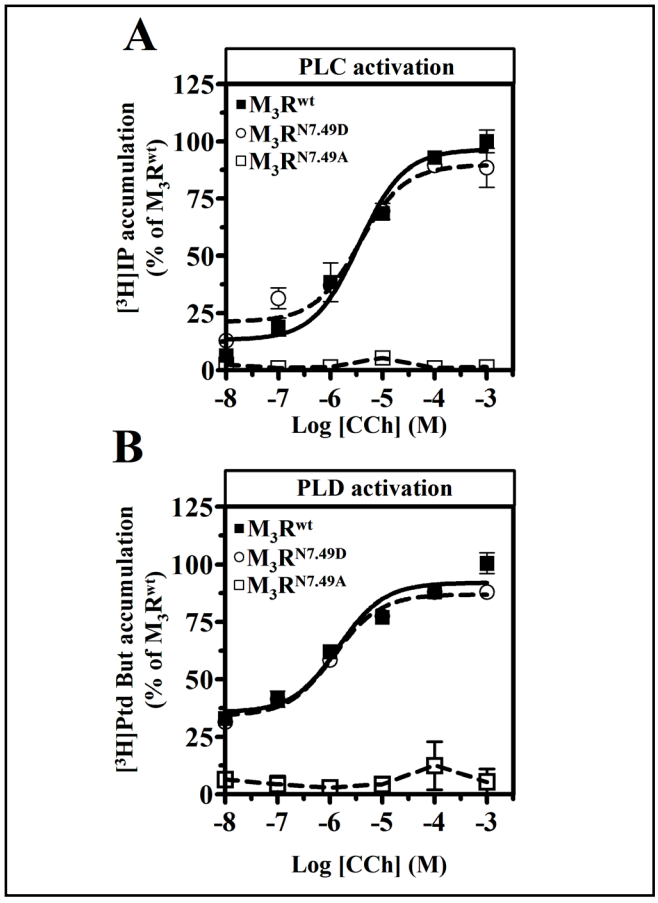

Fig. 2. Activation of PLC and PLD by M_3R constructs in COS-7 cells. COS-7 cells were transiently transfected with the cDNAs encoding M_3R^{wt} (■), $M_3R^{N7.49D}$ (○) and $M_3R^{N7.49A}$ (□) and the IP (A) and PtdBut (B) accumulation after stimulation with increasing concentrations of CCh was determined as described in Materials and Methods. Data are presented as an increase in IP and PtdBut above basal levels in the presence of CCh and referred to the maximal activation produced by M_3R^{wt}. Basal levels observed with the various receptor constructs were not significantly different. Data represents the average ± S.E.M. values of triplicate determinations of three independent experiments.

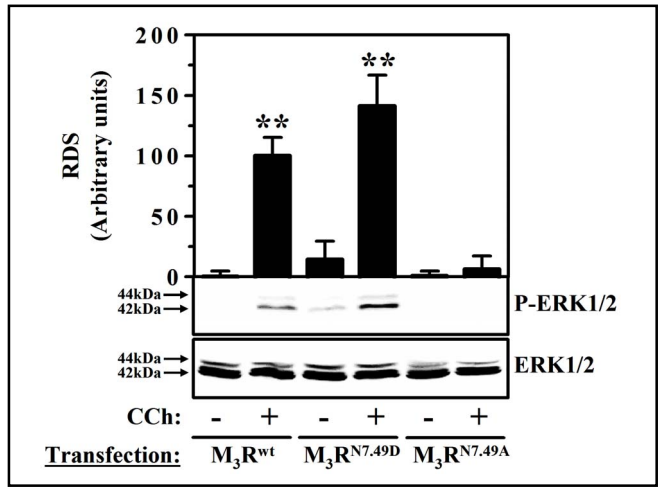

Fig. 3. Stimulation of ERK1/2 by M_3R constructs in COS-7 cells. COS-7 cells were transiently transfected with the cDNAs encoding M_3R^{wr}, $M_3R^{N7.49D}$ and $M_3R^{N7.49A}$ and serum deprived for 12 h before adding CCh (10 μM) for 5 min. Then, cells were washed and processed for MAPK phosphorylation assay (see Materials and Methods). Unphosphorylated and phosphorylated p42 and p44 MAPKs forms were detected using a rabbit anti-ERK1/2 polyclonal antibody and a mouse anti-phospho-ERK1/2 monoclonal antibody, respectively. Immunoreactive proteins were detected using a horseradish peroxidase-conjugated secondary antibody and enhanced chemiluminescences. The intensity of the bands was quantified using Imagen Quand Program (top). Bars represent the means ± S.E.M. of phosphorylated ERK1/2 (P-ERK1/2) normalized using ERK1/2 and expressed as the percentage of change over the M_3R^{wt} level. Results were calculated from five separate experiments. **p<0.001 when compared to unstimulated M_3R^{wt}. RDS, relative densitometric scanning.

Next, we decided to test whether the M_3R mutations impinge into the receptor-mediated MAPK pathway activation. It is well-known that M_3R can activate the MAPK pathway by two ways one that is dependent of protein kinase C and the other independent [28, 29]. Thus, we first assessed whether the M_3R^{wt} transiently expressed in COS-7 cells was able to activate MAPK in response to CCh. A time course analysis of M_3R^{wt}-mediated ERK1/2 phosphorylation using 10 μM CCh reveals a maximal activation at 5 min. Therefore, under these experimental conditions we analyzed all M_3R construct. Interestingly, while the M_3R^{wt} and the $M_3R^{N7.49D}$ were able to induce a clear and consistent ERK1/2 phosphorylation the $M_3R^{N7.49A}$ was unable to trigger a significant ERK1/2 phosphorylation when compared to the other two constructs (Fig. 3).

The $M_3R^{N7.49A}$ couples to but do not activate $G\alpha_{q/11}$

One intriguing question stills the fact that $M_3R^{N7.49A}$ was unable to activate PLC and PLD. Previous studies demonstrated that M_3R activates PLC mainly via a $G\alpha_{q/11}$ and PLD via a $G\alpha_{12/13}$ [27]. Thus, it might be the case that this construct have a lesser affinity for G proteins and when transiently expressed in COS-7 cells it is unable to couple/activate the endogenous G proteins. Consequently, we proceed to coexpress our M_3R constructs with $G\alpha_{q/11}$ and $G\alpha_{12/13}$ in COS-7 cells and check for their functionality. In our hands, co-expression of both $G\alpha_{q/11}$ or $G\alpha_{12/13}$ subunits with the M_3R^{wt} and the $M_3R^{N7.49D}$ increased [^{3}H]IP and [^{3}H]-PtdBut

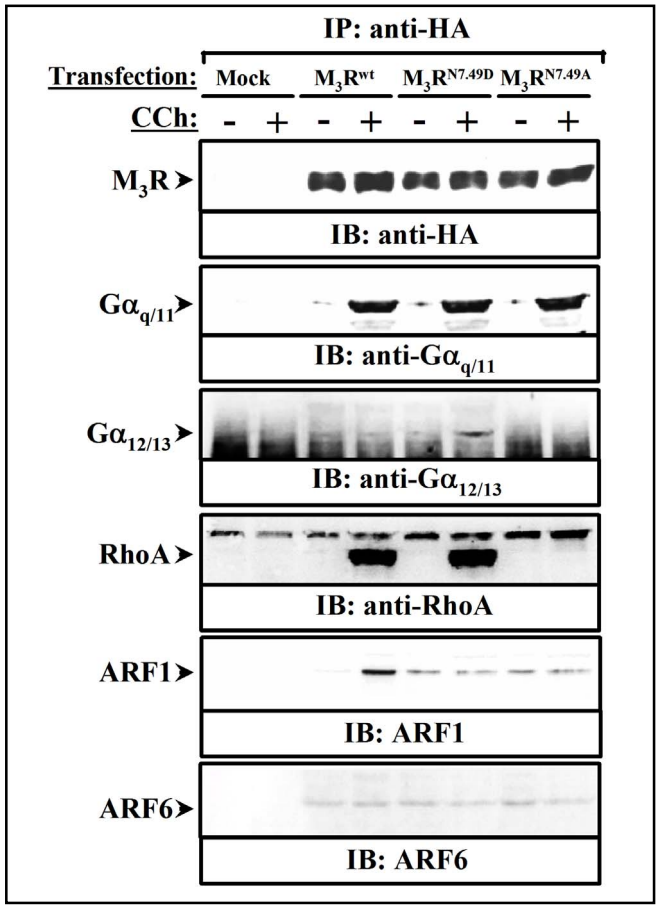

Fig. 4. Association of M_3R constructs with $G\alpha_{q/11}$, $G\alpha_{12/13}$, RhoA, ARF1 and ARF6 proteins. COS-7 cells were transiently transfected with the cDNAs (1 µg) encoding the untagged GPR37 receptor (Mock), 3xHA-M_3R^{wt}, 3xHA-$M_3R^{N7.49D}$ and 3xHA-$M_3R^{N7.49A}$ plus $G\alpha_{q/11}$, $G\alpha_{12/13}$, $RhoA^{GFP}$, $ARF1^{GFP}$ or $ARF6^{GFP}$. Cells were incubated in the absence or presence of 10 µM of CCh for 10 min, solubilized and immunoprecipitated with a mouse anti-HA monoclonal antibody (see Materials and Methods). The immunoprecipitates were subjected to SDS-PAGE and Western blotting analysis using goat anti-HA polyclonal antibody, rabbit anti-$G\alpha_{q/11}$ polyclonal antibody, rabbit anti-$G\alpha_{12/13}$ polyclonal antibody, and rabbit anti-GFP polyclonal antibody to detect $RhoA^{GFP}$, $ARF1^{GFP}$ and $ARF6^{GFP}$. Similar qualitative results were obtained in four independent experiments.

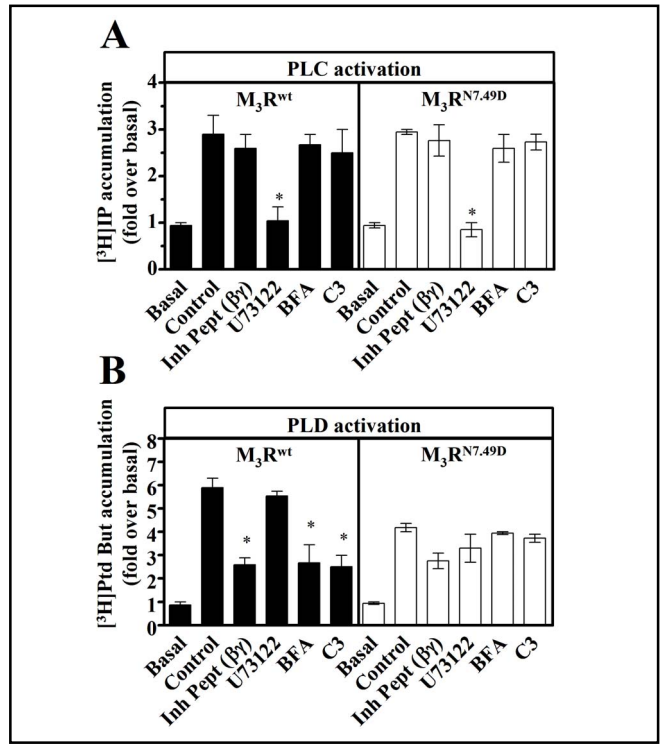

Fig. 5. Characterization of agonist-mediated PLC and PLD activation in COS-7 cells expressing M_3R^{wt} and $M_3R^{N7.49D}$. COS-7 cells transiently transfected with the cDNAs encoding M_3R^{wt} and $M_3R^{N7.49D}$ were stimulated with 10 µM CCh during 10 min in the absence (Control) or the presence of a $G_{\beta\gamma}$ subunit inhibitory peptide (co-transfection with plasmid pREP4-GRK2-Ct), U73122 (15 µM), brefeldin A (BFA, 100 µM) and C3 exoenzyme (C3, 4-8 µg/ml) as described in Materials and methods. The IP (A) and PtdBut (B) accumulations were determined as described in above. In control and inhibitor-treated cells, empty vector equivalent to that used for pREP4-GRK2-Ct was contransfected with the receptor constructs. Values are mean ± S.E.M. (n=5). *$p<0.05$.

accumulation in a concentration dependent manner and that reached a maximum when cells were transfected with 5 µg of the respective Gα DNA plasmids. Under these experimental conditions, when the $M_3R^{N7.49A}$ was co-expressed with either Gα subunits we did not observed PLC nor PLD activation, in agreement with our previous results (Fig. 2). Besides that the $M_3R^{N7.49A}$ did not activate PLC and PLD we wanted to explore if this receptor mutant was able to directly activate Gα proteins, thus we proceeded to check basal guanine nucleotide exchange, using a [^{35}S]GTPγS assay. Therefore, COS-7 cells were transiently transfected with the M_3R^{wt}, the $M_3R^{N7.49D}$ and the $M_3R^{N7.49A}$ and challenged with 10 µM of CCh. Interestingly, while in cells transfected with the M_3R^{wt} and the $M_3R^{N7.49D}$ the agonist challenge induced a clear increase in [^{35}S]GTPγS binding (~43% over basal for all two constructs) in the cells transfected with the $M_3R^{N7.49A}$ no change in [^{35}S]GTPγS binding was observed after CCh challenge. Thus, these results clearly demonstrated that the $M_3R^{N7.49A}$ is unable to activate both endogenous and overexpressed Gα proteins.

Finally, in order to elucidate if the lack of $M_3R^{N7.49A}$-mediated Gα protein activation was due to the loss of receptor-Gα protein interaction we performed co-

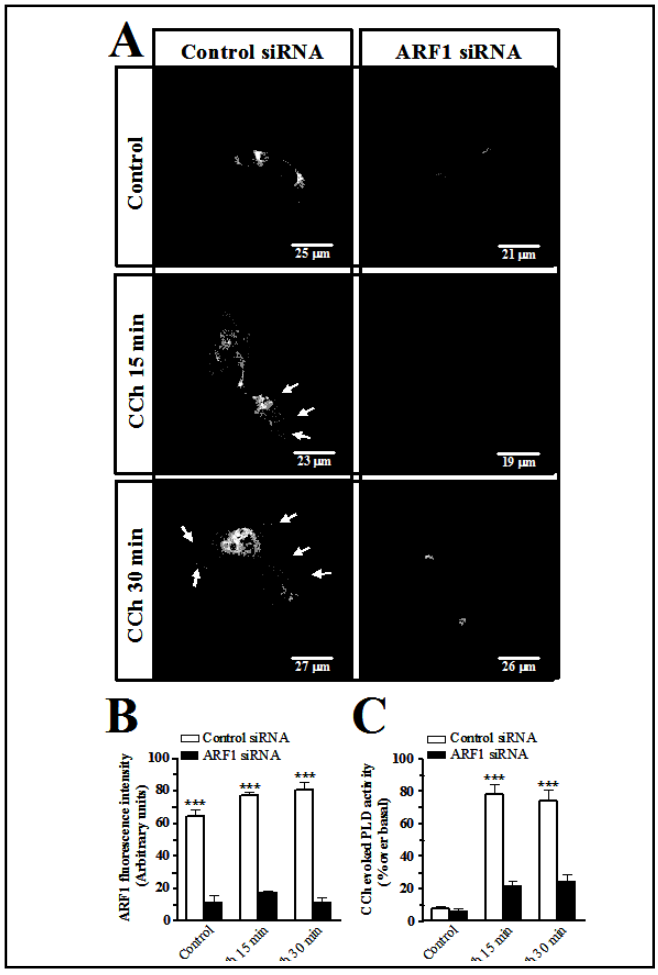

Fig. 6. The M_3R-mediated PLD activation is markedly impaired in ARF1-depleted COS-7 cells. A. COS-7 cells were transfected with M_3R (1 µg) together with a pool of ARF1 siRNA or siRNA negative control (20 µM). 48 hours after transfections cells were serum-starved for 1 h and incubated in presence or absence of CCh (10 µM) for the indicated time. Cells were then fixed and processed for ARF1 immunostaining (see Materials and Methods). Distribution in the control and ARF-1 siRNA transfected cells was examined by confocal microscopy. Left panel illustrates the plasma membrane/cytosolic distribution of the ARF-1 before and after agonist-activation; right panel shows the reduction in the ARF-1 immunofluorescence in ARF1-depleted cells before and after agonist incubation. Arrows denote the plasma membrane distribution of ARF1. This figure is representative of the results obtained in two independent experiments. B. Quantitative ARF-1 immunofluorescence defined as the average fluorescence intensity in a constant field. The data represent the mean ± S.E. of 2 independent experiments (ten images). Statistical significance was determined using Two way ANOVA (PRISM software) (***, $p < 0.001$). C. Agonist-induced PLD activation in control or ARF1-depleted COS-7 cells. Cells, transiently expressing the M_3R, were treated with 10 µM of CCh for 15 and 30 min. The data represent the mean ± S.E. of three independent experiments. Statistical significance was determined using Two way ANOVA (PRISM software) (***, $p < 0.001$).

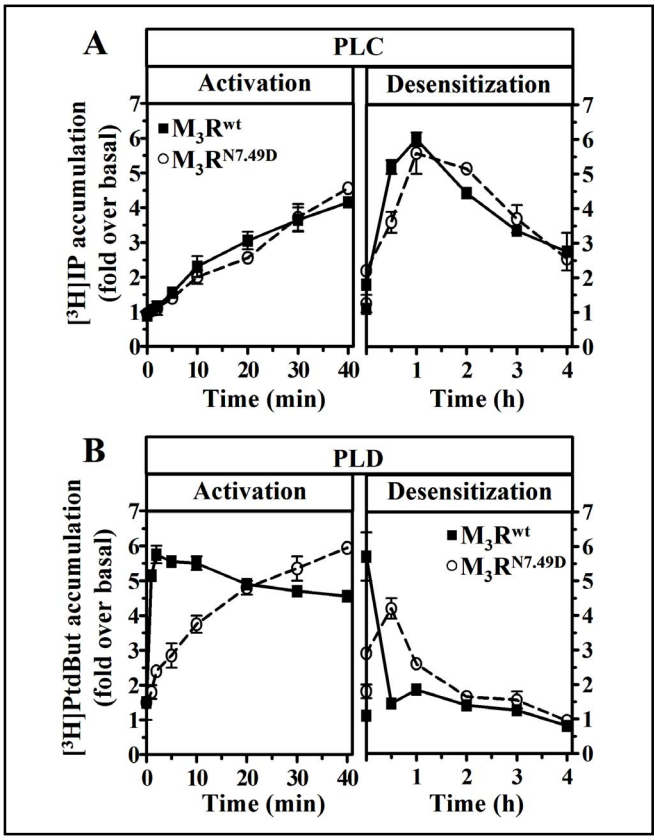

Fig. 7. Characterization of M_3R^{wt}- and $M_3R^{N7.49D}$-mediated PLD and PLC activation/desensitization. A. PLC activation/desensitization time-course. COS-7 cells were transiently transfected with M_3R^{wt} (■) and $M_3R^{N7.49D}$ (○) and the [^{3}H]IP accumulation after CCh (10 µM) challenge was measured at different activation time points (left panel). In addition, cells were pretreated (desensitized) for 2 min with 1 mM CCh (right panel). After washing the cells, a second agonist challenge (10 µM CCh) at the indicated time was performed and the induced [^{3}H]IP accumulation was measured (see Materials and Methods). Values are expressed as fold over basal (mean ± S.E.M. performed in triplicate) of four to six independent experiments. B. PLD activation/desensitization time-course. COS-7 cells were transiently transfected as in panel A and the [^{3}H]PtdButP accumulation after CCh (1 mM) challenge was measured at different activation time points (left panel). In addition, cells were pretreated (desensitized) for 2 min with 1mM CCh (right panel). After washing the cells, a second agonist challenge (10 µM CCh) at the indicated time was performed and the induced [^{3}H]PtdButP accumulation was measured (see Materials and methods). Values are expressed as fold over basal (mean ± S.E.M. performed in triplicate) of four to six independent experiments.

immunoprecipitation experiments in COS-7 cells coexpressing the M_3R^{wt}, the $M_3R^{N7.49D}$ and the $M_3R^{N7.49A}$ together with $G\alpha_{q/11}$ and $G\alpha_{12/13}$. Thus, in cells cotransfected with the M_3R^{wt} and $G\alpha_{q/11}$ the agonist

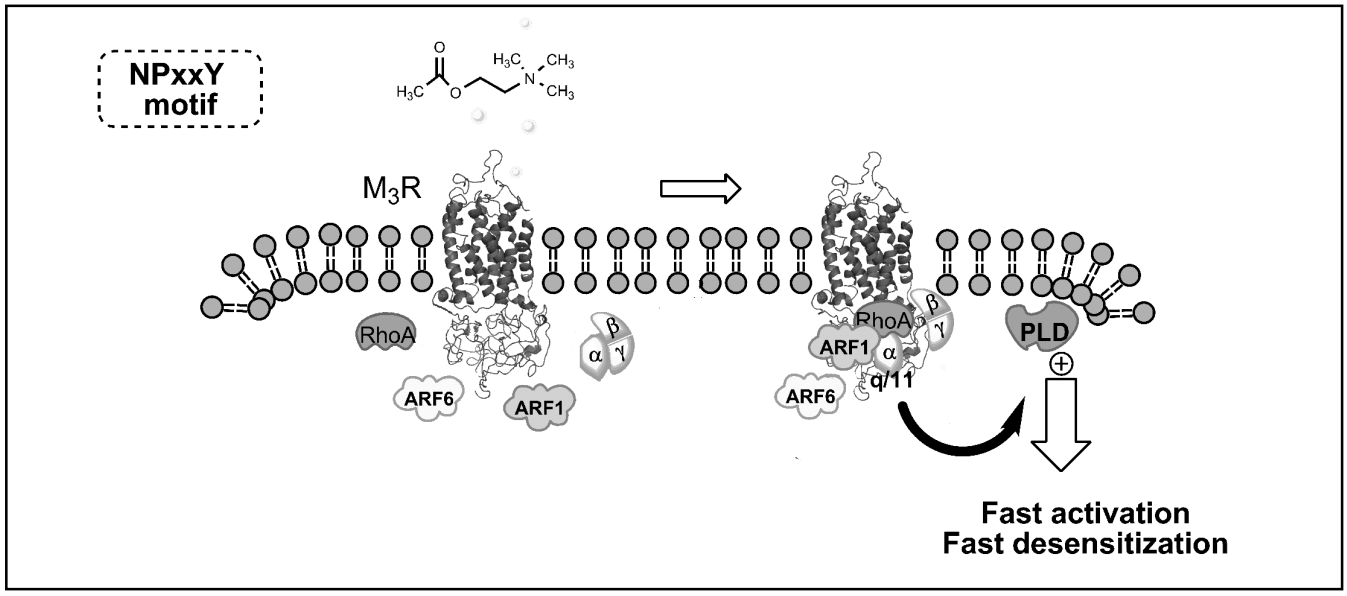

Fig. 8. Schematic representation of the proposed role of the Asn-7.49 in the M_3R signalling complex formation. The signal transduction complex associated with the M_3R, which contains the NPxxY motif, is shown. The receptor modulates PLD activity mainly by the $G\alpha_{q/11}$/ARF1/RhoA/βγ subunit signaling complex, thus a fast activation and desensitization of PLD might be achieved after CCh challenge.

challenge (10 μM of CCh) promoted the interaction of the receptor with the G protein as a band that migrated at 42 kDa corresponding to the $G\alpha_{q/11}$ was clearly coimmunoprecipitated using an antibody against the receptor (Fig. 4). Interestingly, when the $M_3R^{N7.49D}$ and the $M_3R^{N7.49A}$ were immunoprecipitated after agonist treatment it was clear that $G\alpha_{q/11}$ was coimmunoprecipitated with these two receptor constructs. These results show that the $M_3R^{N7.49A}$ binds $G\alpha_{q/11}$ after agonist challenge. Subsequently, similar experiments were performed to check the receptor association with $G\alpha_{12/13}$. A faint basal association of the M_3R^{wt} and the $M_3R^{N7.49D}$ to the $G\alpha_{12/13}$ was observed (Fig. 4). Interestingly, this basal association with the $G\alpha_{12/13}$ protein was unaltered by agonist challenge in the cells expressing the M_3R^{wt} but was increased (~5 fold over the basal) in the cells transfected with the $M_3R^{N7.49D}$ and challenged with CCh (Fig. 4). Under these experimental conditions the $M_3R^{N7.49A}$ did not show any association with the $G\alpha_{12/13}$ even after agonist challenge (Fig. 4). Overall, these results demonstrated that the $M_3R^{N7.49A}$ associated with $G\alpha_{q/11}$ in a similar way as to the M_3R^{wt}, however this association was not sufficient to activate it, thus suggesting that Asn-7.49 is specifically involved in the M_3R-mediated $G\alpha_{q/11}$ protein activation. Also, the Asn→Asp substitution within the NPxxY promoted the association of M_3R^{wt} to $G\alpha_{12/13}$.

The Asn-7.49 plays a key role in the agonist-mediated receptor association with and signals by small monomeric G proteins

In order to elucidate the role of Asn-7.49 in the mechanism of M_3R signaling through small monomeric G proteins we performed coimmunoprecipitation experiments with the ARF and RhoA proteins as these have been described to partake in the receptor signal transduction [16, 18, 19, 30]. Consequently, in cells cotransfected with the M_3R^{wt} and $RhoA^{GFP}$ the agonist challenge promoted the receptor-RhoA interaction as a band that migrated at 50 kDa corresponding to the $RhoA^{GFP}$ was coimmunoprecipitated using an antibody against the HA tag present in all the M_3R constructs (Fig. 4). Interestingly, while the $M_3R^{N7.49D}$ was also able to interact with RhoA after agonist challenge the $M_3R^{N7.49A}$ did not show association with RhoA, thus corroborating again the ineffectiveness of $M_3R^{N7.49A}$ to couple to the canonical $G\alpha_{12/13}$/Rho signaling pathway. Subsequently, similar coimmunprecipitation experiments were performed with ARFs proteins. Thus, in cells cotransfected with the M_3R^{wt} and ARF1 the agonist challenge promoted a significant receptor-ARF1 association that was not observed with either the $M_3R^{N7.49D}$ or $M_3R^{N7.49A}$ (Fig. 4). Interestingly, in cells cotransfected with the M_3R^{wt}, the $M_3R^{N7.49D}$ and the $M_3R^{N7.49A}$ plus ARF6 the agonist treatment was unable to promote the association of these receptor constructs with ARF6 (Fig. 4). Finally, no co-

immunoprecipitation of these small G proteins was observed when an HA untagged GPR37 receptor was used in our experiments as a control (Fig. 4, Mock). Collectively, our coimmunoprecipitation experiments allowed us to show that ARF1 and ARF6 are constitutively associated with the M_3R and that the carbachol challenge promoted the coupling of RhoA and ARF1 with the receptor. Overall, it can be concluded that ARF1 is switched to $G\alpha_{12/13}$ as NPxxY is mutated to DPxxY.

Next, we pharmacologically characterized the agonist-mediated PLC and PLD activation in COS-7 cells expressing M_3R^{wt} and $M_3R^{N7.49D}$ by means of a panel of specific inhibitors. Thus, the M_3R^{wt} and the $M_3R^{N7.49D}$-mediated PLC activation was equally blocked by the U73122, an inhibitor of PLC-dependent processes [31] (Fig. 5A). Interestingly, the M_3R^{wt} and the $M_3R^{N7.49D}$-mediated PLC activation was not inhibited by brefeldin A (BFA), an inhibitor of guanine-nucleotide exchange in ARF [32]; by C3 exoenzyme from *Clostridium botulinum* which inactivates Rho family members (i.e. RhoA) by means of covalent ADP-ribosylation [33]; and by coexpression with the C-terminal tail of the GRK2, which acts as G protein βγ-subunit scavenger [34] (Fig. 5A). These results demonstrated that the Asn→Asp substitution at the conserved NPxxY motif do not affect the PLC activation pattern. On the other hand, M_3R^{wt}-mediated PLD activation was sensible to BFA, to C3 exoenzyme and to the inhibitory G protein βγ peptide (Fig. 5B). These results suggest that the small G proteins (e.g. ARF1/6 and RhoA) and the G protein subunits βγ are involved in the PLD activation, thus illustrating a cross-talk between heterotrimeric and monomeric G-proteins. Interestingly, the $M_3R^{N7.49D}$-mediated PLD activation was not blocked by either BFA, C3 exoenzyme or the inhibitory G protein βγ peptide (Fig. 5B), thus suggesting that the Asn-7.49 play a key role in the ARF/Rho/βγ subunit-mediated PLD activation. Overall, these results agree with the current notion that during agonist activation the M_3R suffers a conformation change that allows the selective translocation/activation of ARF1/RhoA/βγ subunit to the plasma membrane and thus promoting the activation of PLD and controling the PLD desensitization process.

To further confirm the role of ARF1 in the M_3R-mediated PLD activation, we studied PLD activity in ARF1-deficient cells. To this end, a pool of six different double-stranded siRNAs targeting ARF-1 was used to knock down the ARF1 expression in COS-7 cells. Firstly, by means of immunofluorescence and confocal miscroscopy observations we confirmed that the transfection of the ARF1 siRNA, but not the control siRNA, largely reduced (~85%) the ARF1 expression in COS-7 cells (Fig. 6A-B). In addition, when the subcellular distribution of ARF1 was analyzed in control cells (transfected with the control siRNA) we found mostly a cytosolic distribution of the ARF-1 protein that was almost undetectable in ARF1 siRNA transfected cells (Fig. 6A). Interestingly, when cells were challenge with CCh the ARF1 protein showed a more plasma membrane/cytosolic subcellular distribution (Fig. 6A) which again was almost undetectable in cells transfected with ARF1 siRNA (Fig. 6A). In addition, it is noticeable that CCh incubation promoted a marked change in the cellular shape, probably as result of a cell cytoskeleton rearrangement (Fig. 6A), as it has been previously demonstrated [35]. Indeed, a canonical Rho-mediated cytoskeletal rearrangement has been described [36]. Next, under these experimental conditions (i.e. ARF-1 siRNA transfection) we assessed the ability M_3R to activate PLD after agonist challenge. Thus, transiently transfect COS-7 cells were incubated with 10 μM CCh for 15 and 30 min and the PLD activity measured. Interestingly, the activation of PLD following CCh stimulation was dramatically reduced in the cells cotransfected with the ARF-1 siRNA (Fig. 6C). However, when cells were cotransfected with the control siRNA a significant increased in the PLD activity was observed after 15 and 30 min of CCh incubation (Fig. 6C). Overall, these data further support the idea that ARF1, probably at the plasma membrane, specifically regulates M_3R-mediated PLD activation.

The $M_3R^{N7.49D}$ displays an unlike PLD activation time-course and desensitization profile

The agonist challenge of the M_3R activates both PLC and PLD by means of different molecular mechanisms and time kinetics [3], thus, we decided to study the PLC/PLD activation time-course and desensitization profile for the M_3R^{wt} and the $M_3R^{N7.49D}$. Initially, experiments of time-course activation of PLC showed that the M_3R^{wt} and the $M_3R^{N7.49D}$ shared a similar PLC activating profile after CCh challenge (Fig. 7A, left panel). It is important to mention here that the time-course of CCh-stimulated IP accumulation in cells expressing the M_3R^{wt} and the $M_3R^{N7.49D}$ reached a peak around 40 minutes after agonist exposure. On the other hand, a 2 min preexposure of the M_3R^{wt} and the $M_3R^{N7.49D}$ to 1 mM of CCh induced an acute sensitization of the receptor-mediated PLC activation (~6 fold over the basal after 1 hour of the initial 2 min agonist challenge), as previously described in HEK cells [22]. Overall, no obvious differences in the PLC

activation time-course and desensitization profile between the M_3R^{wt} and the $M_3R^{N7.49D}$ were observed.

Next, we performed time-course experiments of receptor-mediated PLD activation. Thus, the M_3R^{wt} showed a pattern of PLD activation with a maximal peak after ~5 min of agonist incubation, followed by a stable plateau (Fig. 7B, left panel). Interestingly, the $M_3R^{N7.49D}$ showed an unlike PLD activation profile that was more similar to that observed for the activation of PLC, thus reaching a maximal peak between 40 to 60 minutes after agonist exposure (Fig. 7B, left panel). On the other hand, a 2 min agonist preexposure of the M_3R^{wt} induced a rapid and persistent desensitization of the receptor-mediated PLD activation (Fig. 7B, right panel), as previously described [22]. Interestingly, the $M_3R^{N7.49D}$ showed a PLD desensitization profile more similar to the one observed for the PLC, thus the 2 min agonist preexposure induced an acute sensitization of the receptor-mediated PLD activation (~4 fold over the basal after 30 min) (Fig. 7B, right panel). These results indicate that there are differences in the kinetics of the receptor-mediated PLD activation/desensitization between the $M_3R^{N7.49D}$ and the M_3R^{wt}. However, there is not a clear explanation for these differences. Thus, the $M_3R^{N7.49D}$-mediated PLD activation pattern resembles the one observed for the receptor-mediated PLC activation/desensitization. Interestingly, as the $M_3R^{N7.49D}$ lacks the carbachol-mediated receptor-ARF1 association it could be proposed that the fast activation and fast desensitization of the M_3R-mediated PLD activation is ARF1 dependent (Fig. 8). Therefore, it might be speculated that M_3R^{wt} can activate PLC and PLD through a signaling complex (e.g. $G\alpha_{q/11}$/$G\alpha_{12/13}$/ARF1/RhoA/$\beta\gamma$ subunit) that might be different to that used by the $M_3R^{N7.49D}$. Overall, the Asn→Asp substitution at the conserved NPxxY motif determines the receptor-G protein switching mode and specificity of the effector activation (e.g. PLC and PLD).

Discussion

Sequence alignment of class A GPCRs reveals that most of its members contain the NPxxY motif [37]. Interestingly, mutagenesis experiments along this domain have been shown to affect the receptor's ligand affinity, expression, G protein-coupling, association with small G proteins and endocytosis [10-13, 38]. As the M_3R also contains this NPxxY motif at the end of it seven transmembrane domain (Fig. 1) we wanted to know the precise role of this motif in receptor functioning. Consequently, to address this question we used site direct mutagenesis in combination with coimmunoprecipitation experiments and signal transduction assays. Thus, this study demonstrates for the first time that the Asn-7.49 of the M_3R NPxxY motif plays a key role in the carbachol-mediated ARF1 association and PLD activation.

Our results are in line with previous studies demonstrating that some residues located within transmembrane helix 7 of certain GPCRs while not being directly implicated in ligand-binding they are involved in the receptor signal transduction. Indeed, during the agonist-mediated conformational rearrangement the residues forming the NPxxY motif are key positions in hydrogen bound formation through receptor stabilization [12, 39, 40]. In our hands, in the M_3R the Asn→Ala substitution (N7.49A point mutation) resulted in a significant decrease in the antagonist maximum binding capacity and an increase in the agonist affinity. A potential explanation would be that the nature of the physicochemical change involved in Asn to Ala mutation somehow affects the hydrogen bond formation essential for keeping the receptor in a stable conformation during activation. Interestingly, Ala replacement at position N7.49 in rhodopsin and in the formyl peptide receptor (FPR) while not promoting a conformational reorganization of the active state of the receptor it implicated a variable change in agonist/antagonist affinity when compared to the wild type receptor [10, 12]. On the other hand, the M_3R Asn→Asp substitution (N7.49D point mutation) did not affect the agonist/antagonist binding properties of the receptor, thus suggesting that this change in charge did not affect the receptor ligand binding properties. In addition, the N7.49A/D M_3R mutants provided further information concerning the receptor's downstream signal transduction. Thus, while the N7.49D point mutation did not affect the affinity and efficacy of the receptor-mediated PLC and PLD activation the N7.49A one precluded the receptor to activate both phospholipases. A comparable functional result was observed when the MAPK pathway was analyzed, thus the $M_3R^{N7.49A}$ mutant was unable to elicit a significant ERK1/2 phosphorylation. Overall, while the change of Asn by Asp maintains a relatively stable conformation of the receptor and does not substantially perturb the conformational change produced during receptor activation the Asn→Ala substitution precluded the receptor-mediated signal transduction.

Our coimmunoprecipitation studies with monomeric small and heterotrimeric G proteins grant some insight about the M_3R signal transduction mechanism. First, we showed that M_3R constitutively associated with $Gq_{/11}$,

ARF1 and ARF6 (Fig. 4) and that agonist challenge promoted the coupling of $G\alpha_{q/11}$, RhoA and ARF1 with the receptor (Fig. 8). In addition, the M_3R^{wt}-mediated PLC activation was inhibited by U73122 and the PLD activation by BFA, by C3 exoenzyme and by a G protein βγ-subunit scavenger. Hence, a major signal transduction complex containing $G\alpha_{q/11}$, ARF1, RhoA and G protein βγ-subunit was depicted (Fig. 8). Next, when the Asn-7.49 of the M_3R NPxxY motif was substituted for Ala (N7.49A point mutation) despite a constitutive faint basal association with ARF1/6 and an agonist-promoted $G\alpha_{q/11}$ coupling was observed the $M_3R^{N7.49A}$ was unable to associate to $G\alpha_{12/13}$ and to RhoA, and thus to activate both PLC and PLD. Finally, the Asn→Asp substitution although did not affect the agonist-mediated receptor association with $G\alpha_{q/11}$ and RhoA it precluded the agonist-mediated receptor-ARF1 association and favored the $G\alpha_{12/13}$ coupling. Interestingly, this unusual receptor coupling pattern did not affect to the PLC activation but it had a profound effect on the PLD stimulation, thus being now insensitive to the G protein βγ-subunit scavenger and to the monomeric small G proteins inhibitors (e.g. BFA and C3 exoenzyme). In addition, our coimmunoprecipitation experiments clearly demonstrated that the N7.49D mutant retains an intact capacity to form stable complexes with RhoA in response to CCh (Fig. 4), thus the formation of high affinity M_3R-RhoA complexes is not sufficient to activate PLD in a RhoA-dependent manner (Fig. 5B, right panel), and consequently, it can be assumed that RhoA is not involved in the $M_3R^{N7.49D}$-mediated PLD activation. Overall, the Asn-7.49 of the M_3R NPxxY motif is specifically involved in the CCh-mediated ARF1 association and in the RhoA-mediated PLD activation.

Previous studies reported that a N376 to D mutation in the conserved NPxxY motif of the 5-HT_{2A} receptor alters the coupling preference from ARF1 to ARF6 [14, 41]. These data suggest that the presence of the N or a D in this highly conserved motif is an important, but not exclusive, determinant of which ARF isoform interacts with the GPCR, since some NPxxY motif-containing receptors such as the M_3R used both isoforms. Our results partially agree with these as the presence of Asp in the M_3R DPxxY motif did not promote the coupling to ARF6, as happens for other receptors, but precluded the agonist-mediated association with ARF1. Interestingly, it has been nicely demonstrted that mutation of the Asn-7.49 of the conserved NPxxY motif of the cholecystokinin B receptor (CCKBR) abolishes $G\alpha_{q/11}$ protein activation without affecting its association with the receptor [11]. In brief, the mutated CCKBR retains an intact capacity to form stable complexes with $G\alpha_{q/11}$ subunits in response to CCK but it was completely unable to mediate activation of either phospholipase C and protein kinase C-dependent and -independent mitogen-activated protein kinase pathways [11], thus indicating that the formation of high affinity CCK-receptor-$G\alpha_{q/11}$ protein complexes is not sufficient to activate $G\alpha_{q/11}$ and suggest that while the Asn-7.49 is specifically involved in $G\alpha_{q/11}$ protein activation other residues might be involved in $G\alpha_{q/11}$ binding [11]. Similarly, we described here that the Asn→Asp substitution within the M_3R NPxxY motif did not affect the association with RhoA but it precluded the small G protein-dependent PLD activation, thus it can be hypothesized that either other residues different than Asn-7.49 might participate in the M_3R-RhoA interaction or that other proteins that act as adapters or regulators of small G protein function may participate or mediate in the association with the receptor. Thus, future studies devoted to clarify the nature of this interaction will determine if RhoA and M_3R interact directly to activate RhoA or if the complex involves other proteins (i.e. ARFs, etc.). Overall, we identified here a single residue within the M_3R sequence that appears to act as a molecular switch for receptor-mediating RhoA activation.

It has been shown that agonist challenge of the M_3R leads to activation of both PLC and PLD but with distinct efficacies and stimulation/desensitization time-courses [22]. However, the essential transducing elements responsible for this differential stimulation/desensitization pattern were not fully identified. Also, it has been demonstrated that the M_3R substantially used an ARF-dependent pathway for PLD activation [30]. Thus, the M_3R displayed a major ARF1-dependent route for PLD1 activation, whereas the ARF6-dependent pathway activates both PLD1 and PLD2 [30]. Nonetheless, the role of ARFs proteins in the M_3R-mediated desensitization of these phospholipases has not been unraveled yet. Our results demonstrated that the Asn-7.49 is essential for grip the M_3R-mediated PLD fast activation and long-lasting desensitization observed in our experiments and also previously reported [22]. This long-lasting M_3R-mediated PLD desensitization suggests that either an inhibitory factor is formed upon receptor activation or that the activated receptor induces the loss or permanent inactivation of an essential coupling component. Indeed, our results also suggest that the Asn-7.49 is necessary for the carbachol-mediated ARF1-receptor association. Thus, we can conclude that the M_3R-mediated PLD fast activation and long-lasting desensitization is ARF1 dependent (Fig. 8). Finally, some members of the GPCR family receptors

exchange the NPxxY motif by DPxxY in TM 7 (i.e. P_{2U} purinergic receptor, PAR, GnRH receptor, etc.) [42], a fact that seems to confer a different pattern of small G proteins activation [14]. Collectively, our results suggest that NPxxY→DPxxY swapping in the M_3R it switch the receptor from one signaling complex (e.g. $G\alpha_{q/11}$/ARF1/RhoA/βγ subunit) to another (e.g. $G\alpha_{q/11}$/$G\alpha_{12/13}$/RhoA). Interestingly, these signal transduction complexes have different PLD activation time-course and desensitization profile.

Abbreviations

M_3R (M_3 muscarinic acetylcholine receptor); GPCR (G protein-coupled receptor); TM (transmembrane helix); H-8 (helix-8); CCh (carbachol); PLC (phospholipase C); PLD (phospholipase D); IP (inositol phosphates); NMS (N-methyl scopolamine).

Acknowledgements

This work was supported by grants from the Swedish Research Council (04X-715), Torsten and Ragnar Söderberg Foundation, Hjärnfonden and Marianne and Marcus Wallenberg Foundation to KF and grants SAF2008-01462 and Consolider-Ingenio CSD2008-00005 from Ministerio de Ciencia e Innovación to FC. FC belongs to the "Neuropharmacology and Pain" accredited research group (Generalitat de Catalunya, 2009 SGR 232) and he is receipted of the ICREA Academia-2010 award from the Catalan Institution for Research and Advanced Studies. We thank Benjamín Torrejón and Esther Castaño from the Scientific and Technical Services (SCT)-Bellvitge Campus of the University of Barcelona for the technical assistance.

References

1 Eglen RM: Muscarinic receptor subtypes in neuronal and non-neuronal cholinergic function. Auton Autacoid Pharmacol 2006;26:219-233.

2 Ishii M, Kurachi Y: Muscarinic acetylcholine receptors. Curr Pharm Des 2006;12:3573-3581.

3 van Koppen CJ, Kaiser B: Regulation of muscarinic acetylcholine receptor signaling. Pharmacol Ther 2003;98:197-220.

4 Borroto-Escuela DO, Ciruela F: Muscarinic receptor-associated proteins: More than just an interaction between proteins; in Ciruela F, Lujan R (eds.): Molecular Aspects of G Protein-Coupled Receptors: Interacting Proteins and Function. Hauppauge, New York, Nova Science Publishers, Inc., 2007, pp. 111-146.

5 Borroto-Escuela DO, Correia PA, Romero-Fernandez W, Narvaez M, Fuxe K, Ciruela F, Garriga P: Muscarinic receptor family interacting proteins: Role in receptor function. J Neurosci Methods 2011;195:161-169.

6 Borroto-Escuela DO, Agnati L, Fuxe K, Ciruela F: Muscarinic acetylcholine receptors interacting proteins (mAChRIPs): Targeting the receptorsome. Curr Drug Targets 2011; in press.

7 Burstein ES, Spalding TA, Brann MR: Amino acid side chains that define muscarinic receptor/G-protein coupling. studies of the third intracellular loop. J Biol Chem 1996;271:2882-2885.

8 Liu J, Blin N, Conklin BR, Wess J: Molecular mechanisms involved in muscarinic acetylcholine receptor-mediated G protein activation studied by insertion mutagenesis. J Biol Chem 1996;271:6172-6178.

9 Wess J, Liu J, Blin N, Yun J, Lerche C, Kostenis E: Structural basis of receptor/G protein coupling selectivity studied with muscarinic receptors as model systems. Life Sci 1997;60:1007-1014.

10 Gripentrog JM, Jesaitis AJ, Miettinen HM: A single amino acid substitution (N297A) in the conserved NPXXY sequence of the human N-formyl peptide receptor results in inhibition of desensitization and endocytosis, and a dose-dependent shift in p42/44 mitogen-activated protein kinase activation and chemotaxis. Biochem J 2000;352:399-407.

11 Gales C, Kowalski-Chauvel A, Dufour MN, Seva C, Moroder L, Pradayrol L, Vaysse N, Fourmy D, Silvente-Poirot S: Mutation of asn-391 within the conserved NPXXY motif of the cholecystokinin B receptor abolishes gq protein activation without affecting its association with the receptor. J Biol Chem 2000;275:17321-17327.

12 Fritze O, Filipek S, Kuksa V, Palczewski K, Hofmann KP, Ernst OP: Role of the conserved NPxxY(x)5,6F motif in the rhodopsin ground state and during activation. Proc Natl Acad Sci USA 2003;100:2290-2295.

13 Kalatskaya I, Schussler S, Blaukat A, Muller-Esterl W, Jochum M, Proud D, Faussner A: Mutation of tyrosine in the conserved NPXXY sequence leads to constitutive phosphorylation and internalization, but not signaling, of the human B2 bradykinin receptor. J Biol Chem 2004;279:31268-31276.
14 Johnson MS, Robertson DN, Holland PJ, Lutz EM, Mitchell R: Role of the conserved NPxxY motif of the 5-HT2A receptor in determining selective interaction with isoforms of ADP-ribosylation factor (ARF). Cell Signal 2006;18:1793-1800.
15 Konvicka K, Guarnieri F, Ballesteros JA, Weinstein H: A proposed structure for transmembrane segment 7 of G protein-coupled receptors incorporating an asn-Pro/Asp-pro motif. Biophys J 1998;75:601-611.
16 Mitchell R, McCulloch D, Lutz E, Johnson M, MacKenzie C, Fennell M, Fink G, Zhou W, Sealfon SC: Rhodopsin-family receptors associate with small G proteins to activate phospholipase D. Nature 1998;392:411-414.
17 Mitchell R, Robertson DN, Holland PJ, Collins D, Lutz EM, Johnson MS: ADP-ribosylation factor-dependent phospholipase D activation by the M3 muscarinic receptor. J Biol Chem 2003;278:33818-33830.
18 Rumenapp U, Geiszt M, Wahn F, Schmidt M, Jakobs KH: Evidence for ADP-ribosylation-factor-mediated activation of phospholipase D by m3 muscarinic acetylcholine receptor. Eur J Biochem 1995;234:240-244.
19 Schmidt M, Voss M, Weernink PA, Wetzel J, Amano M, Kaibuchi K, Jakobs KH: A role for rho-kinase in rho-controlled phospholipase D stimulation by the m3 muscarinic acetylcholine receptor. J Biol Chem 1999;274:14648-14654.
20 Ballesteros JA, Shi L, Javitch JA: Structural mimicry in G protein-coupled receptors: Implications of the high-resolution structure of rhodopsin for structure-function analysis of rhodopsin-like receptors. Mol Pharmacol 2001;60:1-19.
21 Wess J, Gdula D, Brann MR: Site-directed mutagenesis of the m3 muscarinic receptor: Identification of a series of threonine and tyrosine residues involved in agonist but not antagonist binding. EMBO J 1991;10:3729-3734.
22 Schmidt M, Fasselt B, Rumenapp U, Bienek C, Wieland T, van Koppen CJ, Jakobs KH: Rapid and persistent desensitization of m3 muscarinic acetylcholine receptor-stimulated phospholipase D. concomitant sensitization of phospholipase C. J Biol Chem 1995;270:19949-19956.
23 Ciruela F, Burgueno J, Casado V, Canals M, Marcellino D, Goldberg SR, Bader M, Fuxe K, Agnati LF, Lluis C, Franco R, Ferre S, Woods AS: Combining mass spectrometry and pull-down techniques for the study of receptor heteromerization. direct epitope-epitope electrostatic interactions between adenosine A2A and dopamine D2 receptors. Anal Chem 2004;76:5354-5363.
24 Caulfield MP: Muscarinic receptors-characterization, coupling and function. Pharmacol Ther 1993;58:319-379.
25 Schmidt M, Rumenapp U, Keller J, Lohmann B, Jakobs KH: Regulation of phospholipase C and D activities by small molecular weight G proteins and muscarinic receptors. Life Sci 1997;60:1093-1100.
26 Xie Z, Ho WT, Spellman R, Cai S, Exton JH: Mechanisms of regulation of phospholipase D1 and D2 by the heterotrimeric G proteins G13 and gq. J Biol Chem 2002;277:11979-11986.
27 Rumenapp U, Asmus M, Schablowski H, Woznicki M, Han L, Jakobs KH, Fahimi-Vahid M, Michalek C, Wieland T, Schmidt M: The M3 muscarinic acetylcholine receptor expressed in HEK-293 cells signals to phospholipase D via G12 but not gq-type G proteins: Regulators of G proteins as tools to dissect pertussis toxin-resistant G proteins in receptor-effector coupling. J Biol Chem 2001;276:2474-2479.
28 Budd DC, Willars GB, McDonald JE, Tobin AB: Phosphorylation of the Gq/11-coupled m3-muscarinic receptor is involved in receptor activation of the ERK-1/2 mitogen-activated protein kinase pathway. J Biol Chem 2001;276:4581-4587.
29 Novi F, Scarselli M, Corsini GU, Maggio R: The paired activation of the two components of the muscarinic M3 receptor dimer is required for induction of ERK1/2 phosphorylation. J Biol Chem 2004;279:7476-7486.
30 Mitchell R, Robertson DN, Holland PJ, Collins D, Lutz EM, Johnson MS: ADP-ribosylation factor-dependent phospholipase D activation by the M3 muscarinic receptor. J Biol Chem 2003;278:33818-33830.
31 Shi TJ, Liu SX, Hammarberg H, Watanabe M, Xu ZQ, Hokfelt T: Phospholipase C{beta}3 in mouse and human dorsal root ganglia and spinal cord is a possible target for treatment of neuropathic pain. Proc Natl Acad Sci USA 2008;105:20004-20008.
32 Peyroche A, Antonny B, Robineau S, Acker J, Cherfils J, Jackson CL: Brefeldin A acts to stabilize an abortive ARF-GDP-Sec7 domain protein complex: Involvement of specific residues of the Sec7 domain. Mol Cell 1999;3:275-285.
33 Vogelsgesang M, Pautsch A, Aktories K: C3 exoenzymes, novel insights into structure and action of rho-ADP-ribosylating toxins. Naunyn Schmiedebergs Arch Pharmacol 2007;374:347-360.
34 Blackmer T, Larsen EC, Takahashi M, Martin TF, Alford S, Hamm HE: G protein betagamma subunit-mediated presynaptic inhibition: Regulation of exocytotic fusion downstream of Ca^{2+} entry. Science 2001;292:293-297.
35 Slack BE, Siniaia MS: Adhesion-dependent redistribution of MAP kinase and MEK promotes muscarinic receptor-mediated signaling to the nucleus. J Cell Biochem 2005;95:366-378.
36 Leblanc V, Tocque B, Delumeau I: Ras-GAP controls rho-mediated cytoskeletal reorganization through its SH3 domain. Mol Cell Biol 1998;18:5567-5578.
37 Kristiansen K: Molecular mechanisms of ligand binding, signaling, and regulation within the superfamily of G-protein-coupled receptors: Molecular modeling and mutagenesis approaches to receptor structure and function. Pharmacol Ther 2004;103:21-80.
38 Bouley R, Sun TX, Chenard M, McLaughlin M, McKee M, Lin HY, Brown D, Ausiello DA: Functional role of the NPxxY motif in internalization of the type 2 vasopressin receptor in LLC-PK1 cells. Am J Physiol Cell Physiol 2003;285:C750-762.
39 Urizar E, Claeysen S, Deupi X, Govaerts C, Costagliola S, Vassart G, Pardo L: An activation switch in the rhodopsin family of G protein-coupled receptors: The thyrotropin receptor. J Biol Chem 2005;280:17135-17141.
40 Nahorski SR, Tobin AB, Willars GB: Muscarinic M3 receptor coupling and regulation. Life Sci 1997;60:1039-1045.
41 Robertson DN, Johnson MS, Moggach LO, Holland PJ, Lutz EM, Mitchell R: Selective interaction of ARF1 with the carboxy-terminal tail domain of the 5-HT2A receptor. Mol Pharmacol 2003;64:1239-1250.
42 Mirzadegan T, Benko G, Filipek S, Palczewski K: Sequence analyses of G-protein-coupled receptors: Similarities to rhodopsin. Biochemistry 2003;42:2759-2767.